Featured in Physics

First Principles Numerical Demonstration of Emergent Decoherent Histories

Philipp Strasberg, Teresa E. Reinhard, and Joseph Schindler
Física Teòrica: Informació i Fenòmens Quàntics, Departament de Física, Universitat Autònoma de Barcelona, 08193 Bellaterra (Barcelona), Spain

(Received 11 May 2023; revised 1 July 2024; accepted 30 July 2024; published 30 October 2024)

Within the histories formalism the decoherence functional is a formal tool to investigate the emergence of classicality in isolated quantum systems, yet an explicit evaluation of it from first principles has not been reported. We provide such an evaluation for up to five-time histories based on exact numerical diagonalization of the Schrödinger equation. We find a robust emergence of decoherence for slow and coarse observables of a generic random matrix model and extract a finite-size scaling law by varying the Hilbert space dimension over 4 orders of magnitude. Specifically, we conjecture and observe an exponential suppression of coherent effects as a function of the particle number of the system. This suggests a solution to the preferred basis problem of the many-worlds interpretation (or the set selection problem of the histories formalism) within a minimal theoretical framework without relying on environmentally induced decoherence, quantum Darwinism, Markov approximations, low-entropy initial states, or ensemble averages.

DOI: 10.1103/PhysRevX.14.041027

Subject Areas: Cosmology, Quantum Physics, Statistical Physics

I. INTRODUCTION

Do we live in a quantum multiverse? Since the formulation of the many-worlds interpretation (MWI) [1–3], this idea enjoys increasing popularity among researchers [4–6], popular science [7], and pop culture [8]. Although the basic premise of the MWI is "simply" to assume unitary evolution for the entire Universe (including its observers), its seemingly absurd consequence that the Universe consists of many universes existing in parallel (the multiverse) is a source of strong controversies [9]. Using nonrelativistic quantum mechanics, our contribution is to provide direct evidence—within a minimal first principles setup—that the MWI is compatible with our experienced "classical reality."

It is useful to clarify from the start that the idea of the quantum multiverse and the MWI should be distinguished from other potential multiverses based on, e.g., an infinitely large Universe, many inflationary bubbles, different fundamental constants, or various solutions in the string theory landscape [4,10]. Those universes are thought of as being separated in spacetime, and thus admit in principle a classical understanding. In contrast, the multiverse of the MWI consists of different universes at the same spacetime location.

One essential technical problem associated with the MWI is called the preferred basis problem: how to reconcile the multiverse with our perceived classical experience within one universe. If Schrödinger's equation is applied to the entire Universe, then by linearity, superpositions proliferate and spread, splitting the wave function into many universes, or histories, evolving in parallel (also called branches, worlds, realities, narratives, etc.). However, the wave function can—without approximation—be split with respect to many different bases (indeed, a continuum of bases), and each basis provides *a priori* an equally justified starting point (and as we will discuss, the wave function can be also split backward in time). But as Bohr, in endless discussions with Einstein about the double-slit experiment (and others), has made clear, a state describing a superposition of different properties makes said property ontologically indeterminate: In the double-slit experiment, the particle has no meaningful location without measurement [11]. Thus, without identifying an additional structure justifying a classical description, as we experience it, the MWI describes infinitely many ontologically indeterminate splittings: *A priori*, none of them allows us to speak about "histories," "worlds," or "realities" in any conventional, meaningful sense.

This additional structure must be derived within the MWI, and within nonrelativistic quantum mechanics a satisfactory derivation must comply at least with two minimal desiderata. (i) The system is isolated, evolves unitarily, and is prepared in a pure state. This avoids the introduction of any form of classical noise from the outside (e.g., in the form of ensemble averages), which potentially

Published by the American Physical Society under the terms of the Creative Commons Attribution 4.0 International license. Further distribution of this work must maintain attribution to the author(s) and the published article's title, journal citation, and DOI.

implies the answer to the question already from the start. We remark that the system might be (but does not need be) split into subsystems. (ii) The condition of classicality must be a meaningful, rigorous definition that is suitable to account for multitime properties or temporal correlation functions because the perception of classicality is a repeated experience (adapting Einstein's quote, the moon was there yesterday, is there today, and will be there tomorrow). This is important: Speaking of different worlds or histories becomes meaningful if we can reason about their past, present, and future in classical terms.

Here, we use the decoherence functional (DF) introduced within the consistent or decoherent histories framework (or simply, "histories framework" for short) [12–21] to rigorously investigate the emergence of multitime classicality (see Sec. II for the technical details). We numerically show that bases defined by a slow and coarse observable of a nonintegrable system are robustly decoherent according to this criterion. More specifically, we show for up to five-time histories and a Hilbert space dimension D varying over 4 orders of magnitude that quantum effects (suitably quantified below) are exponentially suppressed as a function of the particle number N of the system (with $N \sim \log D$). This provides a firm starting point to discuss the MWI and to address the set selection problem of the histories framework [18,22–24]. Our results also explicitly show that the emergence of classicality is ubiquitous, that almost all initial wave functions can give rise to interesting universes, and that the branching of the wave function is *a priori* not related to any arrow of time.

Perhaps surprisingly, our results do not rely on environmentally induced decoherence (EID) [25–27] (note the unfortunate double meaning of decoherence in the literature: *A priori*, there is no connection between the DF in the histories framework and the concept of EID) or its refinement to quantum Darwinism [28–30]. This is surprising because the widely proclaimed (sole) answer to the question why the MWI gives rise to classically looking universes is EID, and many researchers worked on connecting the MWI or the histories framework with EID and quantum Darwinism [22,24,31–41], yet an explicit evaluation of the DF following the desiderata (i) and (ii) is still missing. Only if one invokes a rigorous notion of multitime quantum Markovianity [42–44], clear connections between the DF and EID have been established [22,33–35,37,41], but this shifts only the problem of proving multitime decoherence to proving multitime Markovianity, which is a daunting task, too [45–49].

In contrast, the present approach does not rely on any system-environment tensor product splitting, although it is important to emphasize that it is not in conflict with EID or quantum Darwinism when applied to it. Instead, we consider only slow and coarse observables of isolated, nonintegrable quantum systems, similar to the approach taken by Van Kampen in 1954 [50]. While the importance of slow and coarse (or quasiconserved) observables for the emergence of decoherence has been anticipated in the histories formalism [16,20,51–56], nonintegrability has never been considered a key factor by proponents of the histories, EID, or quantum Darwinism framework: Van Kampen's work remained ignored despite him emphasizing its importance for the quantum-to-classical transition [57,58]. More precisely, nonintegrability is taken here to mean that random matrix theory captures well the relevant dynamic behavior. While this is known to be true in many situations [59–65], in the context of the quantum-to-classical transition, rigorous evidence for Van Kampen's idea slowly accumulated only recently [41,49,66–68]. Moreover, it has not yet been considered in light of the MWI and a first principles evaluation of the DF remains missing.

To summarize, our objective is to subject the MWI and the question whether it is compatible with our perceived classical reality to a rigorous, quantitative test based on the minimal desiderata (i) and (ii). To this end, we introduce the general theoretical framework to address this question in Sec. II. Then, we present extensive numerical results for a heat-exchange model (an archetypical example of a nonequilibrium process in thermodynamics) in Sec. III. Section IV discusses the set selection problem in view of our findings, and we conclude and provide perspectives in Sec. V.

II. GENERAL FRAMEWORK

A. Mathematical definitions and problem

We consider an isolated quantum system with Hilbert space $\mathcal{H}$ of dimension $D = \dim \mathcal{H}$ and Hamiltonian H. The time-evolution operator from t_j to t_k is denoted $U_{k,j} = e^{-iH(t_k - t_j)}$ ($\hbar \equiv 1$) and the initial state is $|\psi(t_0)\rangle$. Furthermore, $\{\Pi_x\}_{x=1}^M$ denotes a complete set of M orthogonal projectors satisfying $\sum_{x=1}^M \Pi_x = I$ (with I the identity) and $\Pi_x \Pi_y = \delta_{x,y} \Pi_x$. They divide the Hilbert space into a direct sum of subspaces: $\mathcal{H} = \bigoplus_{x=1}^M \mathcal{H}_x$. The dimension of the subspace $\mathcal{H}_x$ equals the rank of the projector Π_x and is denoted $V_x = \mathrm{tr}\{\Pi_x\} = \dim \mathcal{H}_x$. Note that $D = \sum_{x=1}^M V_x$.

Next, we decompose the unitarily evolved state $|\psi(t_n)\rangle = U_{n,0}|\psi(t_0)\rangle$ by writing $U_{n,0} = U_{n,n-1} \cdots U_{1,0}$ and inserting identities at times $t_n > \ldots > t_1 > t_0$:

$$|\psi(t_n)\rangle = \sum_{x_n} \Pi_{x_n} U_{n,n-1} \cdots \sum_{x_1} \Pi_{x_1} U_{1,0} \sum_{x_0} \Pi_{x_0} |\psi(t_0)\rangle \equiv \sum_{\mathbf{x}} |\psi(\mathbf{x})\rangle. \quad (1)$$

Here, we abbreviate $\mathbf{x} = (x_n, \ldots, x_1, x_0)$, which we call a history of length $L = n + 1$ in the following. Moreover, $|\psi(\mathbf{x})\rangle = \Pi_{x_n} U_{n,n-1} \cdots \Pi_{x_1} U_{1,0} \Pi_{x_0} |\psi(t_0)\rangle$ is the (nonnormalized) state conditional on "passing through"

subspaces $\mathcal{H}_{x_j}$ at times t_j. Note that this construction becomes identical to Feynman's path integral if we let $t_{j+1} - t_j \to 0$ and consider projectors Π_x in the position representation.

Finally, we introduce the decoherence functional

$$\mathfrak{D}(\mathbf{x};\mathbf{y}) \equiv \langle \psi(\mathbf{y}) | \psi(\mathbf{x}) \rangle, \tag{2}$$

which is a Hermitian $M^L \times M^L$ matrix. Moreover, the important decoherent histories condition (DHC) is defined by the condition

$$\mathfrak{D}(\mathbf{x};\mathbf{y}) = 0 \quad \text{for all } \mathbf{x} \neq \mathbf{y}. \tag{3}$$

The central task of this work is to understand the conditions when the DHC is generically satisfied. In particular, we will see that it is hard to strictly satisfy Eq. (3) for the situations we are interested in. Hence, we will quantitatively study from first principles a suitable smallness condition $\mathfrak{D}(\mathbf{x};\mathbf{y}) \approx 0$ discussed in Sec. II C below. We remark that this is a well-defined and nontrivial mathematical problem—independent of the physical meaning attached to the different objects to which we turn now.

B. Physical meaning and further terminology

We continue with physical clarifications, also related to the previous literature.

First, we call $\{\Pi_x\}_{x=1}^M$ a coarse-graining and x a macrostate, which is conventional terminology in statistical mechanics. Indeed, we are interested in observables that humans can perceive, and those are necessarily coarse. Quantitatively, this means that the number of projectors is much smaller than the Hilbert space dimension: $M \ll D$. Note that this is also satisfied in any quantum experiment that relies on macroscopic detectors.

Next, we briefly clarify the meaning of the DHC, which has been already discussed in the literature [12–21]. [There has also been some controversy about the precise mathematical formulation of the DHC (see, e.g., Ref. [69]), but it seems that Eq. (3) is nowadays universally accepted [21].] To this end, recall that according to our classical (Newtonian or prequantum) ontology, the world out there is made up of entities with independent and well-defined properties that can be revealed in principle to arbitrary precision; i.e., any uncertainty about the state of the world is entirely subjective or epistemic (for a broader discussion see, e.g., Ref. [11]). This world view is challenged by quantum physics. However, the DHC guarantees that, for the process describing the macrostates x_j at times t_j, such a classical ontology becomes quantitatively accurate because Eq. (3) describes the absence of detectable quantum-interference effects. This makes the dynamics of the coarse properties x_j isomorphic to a classical stochastic process (see also Refs. [41,44,49,70–75]) and implies the validity of Leggett-Garg inequalities [76].

Before turning to the connection with the MWI, it is important to be clear about the fact that the DHC has differing ontological statuses even among practitioners of the histories formalism [14,18]. For instance, Griffiths regards the DHC as primary; that is, quantum evolution is fundamentally stochastic, and the deterministic Schrödinger equation can be used to compute only the DF if the DHC is satisfied [12,19,21]. In contrast, here we take unitary evolution as primary (as in the MWI) and view the DHC as an emergent property. This means we use the histories formalism as a convenient mathematical tool to address a well-defined problem.

We deliberately point out that this attitude shall neither imply that the MWI is correct nor that the consistent histories interpretation of Griffiths is incorrect. In contrast, the question we ask here sheds light on both interpretations. It is important to know for the MWI whether the quantum multiverse supports decoherent histories, and likewise the question with which histories Schrödinger's equation is compatible, and whether this compatibility is exact or approximate, influences the scope of the consistent histories interpretation.

We continue by commenting on the connection between the DHC and the MWI as we view it in this work. As emphasized in the Introduction, the definition of a "world" within the MWI is *a priori* complicated by the existence of a continuum of mathematically conceivable different worlds (preferred basis problem). Moreover, even among the proponents of the MWI there is no universally agreed on quantitative definition of a world (see, e.g., Ref. [77] for a short overview). Here, we use this liberty and interpret the DHC as a minimal criterion to define a world within the MWI. This is motivated by what we said above: The classical world that we perceive is compatible with quantum mechanics precisely when the observables we look at satisfy the DHC. We believe this view is in unison with proponents of the MWI; for instance, Vaidman verbally defines a world as "the totality of macroscopic objects … in a definite classically described state" [3]. Moreover, only past "events" giving rise to decoherent histories can leave records about having "happened" in the present state of the Universe, which highlights the importance of the DHC [16,22,24,31,78–81].

In the following, it is also advisable to drop the word "classical" in favor of "decoherent," at least in a technical context. Indeed, depending on the context, classicality can have many different meanings since the boundary between quantum and classical physics cannot be reduced to a single condition. Thus, in short, our terminology is the following: Histories that satisfy exactly or approximately (see Sec. II C) the DHC are called decoherent (and only sometimes classical), and in the context of the MWI we call those histories also branches or worlds. We also repeat once more that the DHC is not identical to but compatible with the concept of EID.

We conclude by specifying what we mean by a first principles demonstration of the DHC. Essentially, we aim for a general understanding of the DHC by using physical assumptions that are not in conflict with the framework of Sec. II A. This has two major implications. First, we do not allow for any assumption that breaks unitarity and, instead, we solve the Schrödinger equation exactly. In particular, we do not use Markov approximations as done in Refs. [22,33–35,37,41,70,71,73], which—even though insightful—shift the problem from justifying classicality to justifying Markovianity.

Second, we demand that the state of the isolated system is pure. By avoiding classical ensemble averages, any remaining uncertainty must stem from the quantum state or dynamics. Indeed, the only explicit evaluation of the DHC for a nontrivial many-particle system (and not relying on Markov approximations) has been done using the influence functional for a harmonic oscillator environment (Caldeira-Leggett model), assuming that the environment is prepared in a canonical Gibbs ensemble [15,16,79,82–84]. This is problematic, as it remains unclear whether the observed decoherence is a consequence of the dynamics itself (as one would hope for) or a consequence of the classical ensemble average.

What remains beyond Markov approximations and ensemble averages, and beyond conserved quantities that trivially satisfy the DHC, are indirect arguments based on, e.g., the approximate behavior of projectors in the Heisenberg picture [14,16,20,51–56,85]; see also Ref. [86]. But an explicit evaluation of the DHC or even an estimate of it has never been attempted therein. It is this important gap that we fill with the present work, which is backed up by the general idea of Van Kampen [50] (see also Sec. II D) and supported only by a few preliminary results so far [41,49,66–68].

C. Approximate decoherence

For reasons that will become clear below, exact decoherence, i.e., a strict satisfaction of Eq. (3), is not the rule. All we can realistically hope for is to satisfy the DHC approximately, even though our results will also indicate that this approximation is typically so good that it becomes indistinguishable from exact decoherence for all practical purposes.

Approximate decoherence is typically quantified—after realizing $|\mathfrak{D}(\mathbf{x};\mathbf{y})| \leq \sqrt{\mathfrak{D}(\mathbf{x};\mathbf{x})\mathfrak{D}(\mathbf{y};\mathbf{y})}$ due to Cauchy-Schwarz inequality—by introducing a "normalized DF" and demanding that [15]

$$\epsilon(\mathbf{x};\mathbf{y}) \equiv \frac{|\mathfrak{D}(\mathbf{x};\mathbf{y})|}{\sqrt{\mathfrak{D}(\mathbf{x};\mathbf{x})\mathfrak{D}(\mathbf{y};\mathbf{y})}} \ll 1 \quad \text{for all } \mathbf{x} \neq \mathbf{y}. \tag{4}$$

While this is a reasonable, properly normalized condition for smallness, in practice this condition can still be cumbersome. There are $M^{2L-1} - M^L$ many $\epsilon(\mathbf{x};\mathbf{y})$ for histories of length $L = n + 1$ that are not trivially 1 because of $\mathbf{x} = \mathbf{y}$ or trivially zero because of $x_n \neq y_n$ (owing to the orthogonality of the projectors at the final time). Studying all of them becomes unfeasible for large M or L. Moreover, the exact operational meaning of Eq. (4) is at least *a priori* not apparent; i.e., what does it imply for an experimentalist who tries to decide whether a process is decoherent or not?

We therefore choose a dual strategy to quantify decoherence in this work. First, we consider the average of the nontrivial values of $\epsilon(\mathbf{x};\mathbf{y})$ defined as

$$\epsilon \equiv \frac{1}{M^{2L-1} - M^L} \sum_{\mathbf{x}\neq\mathbf{y}} \epsilon(\mathbf{x};\mathbf{y}). \tag{5}$$

This is probably the simplest quantifier one can consider, but we believe its simplicity makes it appealing to get a first impression of what is going on.

However, to rigorously quantify the worst-case scenario in an operationally meaningful way, we also consider a second strategy. To this end, we select an arbitrary subset $T \subset \{t_0, t_1, \ldots, t_n\}$ of times on which the DF is defined, for instance, $T = \{t_2, t_7\}$ in the sketch of Fig. 1. Furthermore, we denote by Z_T all possible histories $\mathbf{z}$ that we can associate with T with respect to the given coarse-graining; e.g., with respect to Fig. 1 these are all two-time histories $Z_T = \{x_7^1, x_7^2, \ldots, x_7^6\} \times \{x_2^1, x_2^2, \ldots, x_2^6\}$ (with $\times$ the Cartesian product).

Next, we construct two types of probabilities on Z_T. The first is the actual Born rule probability to measure $z \in Z_T$, which we can get from the DF defined on T via

$$p(\mathbf{z}) \equiv \sum_{\mathbf{x}(\mathbf{z}),\mathbf{y}(\mathbf{z})} \mathfrak{D}(\mathbf{x};\mathbf{y}), \tag{6}$$

where $\sum_{\mathbf{x}(\mathbf{z})}$ indicates a sum running over all $\mathbf{x}$ holding $\mathbf{z}$ fixed. For instance, for the example in Fig. 1 (the pink bars) we have $\sum_{\mathbf{x}(\mathbf{z})} = \sum_{\mathbf{x}} \delta_{x_7,x_7^3}\delta_{x_2,x_2^4}$ and thus,

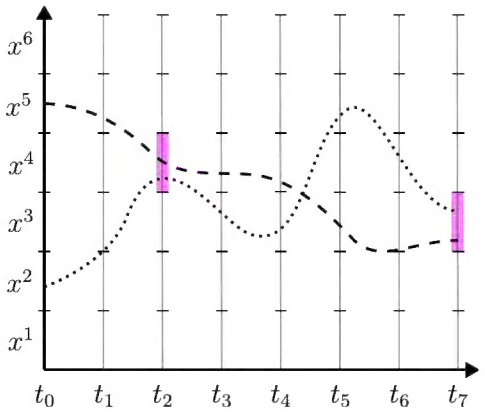

FIG. 1. Example illustrating the DF for a coarse-graining with six macrostates and eight time steps. Two possibly interfering histories are indicated by dashed and dotted lines (the lines are used for visualization only; within this DF only their macrostates at times t_i are defined).

$$p(\mathbf{z}) = \langle\psi(t_0)|U_{2,0}^{\dagger}\Pi_{x_4}U_{7,2}^{\dagger}\Pi_{x_3}U_{7,2}\Pi_{x_4}U_{2,0}|\psi(t_0)\rangle. \tag{7}$$

The second probability we can introduce is a decohered or classical version of $p(\mathbf{z})$ obtained under the assumption that the DHC is obeyed. It is defined as a sum over the diagonal elements only:

$$p_{\mathrm{cl}}(\mathbf{z}) \equiv \sum_{\mathbf{x}(\mathbf{z})} \mathfrak{D}(\mathbf{x};\mathbf{x}). \tag{8}$$

Now, to evaluate the difference between the true quantum probability distribution $p(\mathbf{z})$ and its decohered counterpart $p_{\mathrm{cl}}(\mathbf{z})$ we use the L_1 norm or trace distance

$$\Delta_T(p|p_{\mathrm{cl}}) \equiv \frac{1}{2}\sum_{\mathbf{z}\in Z_T}|p(\mathbf{z}) - p_{\mathrm{cl}}(\mathbf{z})| \in [0,1]. \tag{9}$$

Inserting the definitions, we see that the trace distance is determined by the off-diagonal elements of the DF:

$$\Delta_T(p|p_{\mathrm{cl}}) = \frac{1}{2}\sum_{\mathbf{z}\in Z_T}\left|\sum_{\mathbf{x}(\mathbf{z})\neq\mathbf{y}(\mathbf{z})}\mathfrak{D}(\mathbf{x};\mathbf{y})\right|. \tag{10}$$

In addition, the trace distance has a clear operational meaning in a hypothesis testing scenario [87]. Namely, it determines in an optimized single-shot scenario the minimum probability $P_{\mathrm{min}}(\mathrm{fail}) = [1 - \Delta_T(p|p_{\mathrm{cl}})]/2$ for an experimenter to fail to distinguish between the coherent and decohered quantum process described by $p(\mathbf{z})$ and $p_{\mathrm{cl}}(\mathbf{z})$, respectively. For a given measurement resolution, this $P_{\mathrm{min}}(\mathrm{fail})$ gives the desired criterion to decide when a set of approximately decoherent histories is "decohered enough." However, the trace distance (9) still depends on T, but we are interested only in the worst-case scenario. Moreover, we notice the following fact: If $t_n \notin T$, then the sum over x_n and y_n does not contribute to Eq. (9). This follows from a containment property of the DF: The DF for histories of length $L' < L$ can be obtained from the DF for histories of length L by tracing out the final $L - L'$ time steps. Thus, we will plot in Sec. III the maximum

$$\Delta_L^{\mathrm{max}} \equiv \max_{T\cap\{t_n\}\neq\varnothing}\Delta_T(p|p_{\mathrm{cl}}). \tag{11}$$

Note that this number still depends on L.

D. Physical origin of decoherence

The physical origin of decoherence has been discussed at many places and shall not be repeated here in detail. We therefore limit ourselves to listing the four assumptions used by Van Kampen [50] followed by a perhaps oversimplified yet hopefully intuitive analogy.

The four assumptions are the following. First, one needs a large Hilbert space dimension D, which is certainly satisfied for macroscopic systems. Typically, $D = \mathcal{O}(10^N)$ and $N = \mathcal{O}(10^{23})$ to give some numbers. Second, one must consider a coarse coarse-graining satisfying $M \ll D$. As discussed above, this is satisfied for all that we humans can perceive. Third, the considered projectors must evolve slowly in a suitable sense such that the unobserved microscopic degrees of freedom have time to self-average or randomize. Common examples include hydrodynamic modes, collective degrees of freedom, weakly coupled subsystems, or more generally, projectors that almost commute with the total Hamiltonian (for a more technical discussion about the notion of slowness, see Ref. [49]). Fourth, the isolated system should be nonintegrable.

This last point is certainly still subject to debate, not the least because a universally agreed on definition of quantum (non)integrability is lacking. For instance, Van Kampen assumed that the energy-gap spectrum of the Hamiltonian H is nondegenerate (apart from rare accidental degeneracies) [50], the results of Refs. [49,66–68] were based on the eigenstate thermalization hypothesis [64,65], and here we use random matrix theory as also done in Refs. [41,68]. Since already classical systems tend to be chaotic (e.g., the Newtonian three-body problem), we believe that nonintegrability can hardly count as an assumption in our Universe, even though it is an open question whether it is strictly necessary.

Intuitively, we like to motivate the need for nonintegrability by the following analogy. Since the DHC describes the lack of interference between different macrostates x, we like to picture the coherences of all microscopic degrees of freedom as ripples caused by stones thrown into an initially still pond. If one zooms in very much (corresponding to very large M) or considers only a single stone thrown into the pond (corresponding to very small D), one can certainly see a clear wave pattern and interference effects. But if one zooms out a bit, or averages over a small area of the pond, and throws in a lot of stones (at different places), it becomes very hard to see any significant interference effects. One reason for it is simply the law of large numbers: There are many more combinations possible where ripples from different stones destructively interfere than possible combinations of constructive interference. This is identical to rolling 10^{23} dice: The vast majority of sequences has an average face value around 3.5, and the number of sequences deviating significantly from it is exponentially suppressed. However, there is also another effect at work. In reality, all stones have a slightly different size and weight, thus causing ripples with, e.g., different amplitudes or velocities. This implies that even if at a certain moment in time the state of the stones is highly synchronized (for instance, they could have been thrown symmetrically into the pond), this synchronized state will very quickly dephase and look generic. This effect is absent in integrable systems where the extensive amount of conserved quantities causes many regularities in the dynamics. It is thus reasonable to conjecture that nonintegrable systems, here corresponding

to stones of different sizes and weights, show a more robust emergence of decoherence for a broader class of initial states.

III. NUMERICAL DEMONSTRATION

A. Setup

We will now explicitly validate the idea that coarse and slow observables of a nonintegrable many-body system satisfy the DHC with increasing accuracy for increasing Hilbert space dimension D. This is done by exact numerical diagonalization for a setup consisting of two identical, coupled systems exchanging energy. We choose this archetypical setup of a nonequilibrium thermodynamic process because it is intuitive and allows us to clearly identify arrow(s) of time associated with the flow of heat from hot to cold. In principle, this flow of heat could then be harnessed to create work or free energy, an important prerequisite for the formation of life and intelligent observers in the Universe, but (obviously) our code cannot simulate any forms of life or observers.

We call our systems A and B (see Fig. 2 for a sketch), and the total Hamiltonian is

$$H = H_A + H_B + \lambda H_I, \tag{12}$$

where H_I is the interaction and λ a small parameter to ensure weak coupling (see below). We coarse-grain the local energies of A and B by projectors $\Pi_{x,x'} \equiv \Pi_x^A \otimes \Pi_{x'}^B$ for a pair of integers (x, x'). In units of some energy precision or width ΔE, $\Pi_{x,x'}$ projects on the energy interval $[x, x+1) \times [x', x'+1)$; i.e., Π_x^A is spanned by all energy eigenstates $|k\rangle_A$ of H_A whose energy eigenvalue E_k satisfies $x \leq E_k/\Delta E < x+1$, and similarly for $\Pi_{x'}^B$.

In the following, we consider one microcanonical subspace with some fixed total energy $E_{\text{tot}} = E_A + E_B$, where E_A (E_B) is the coarse-grained energy of system A (B) determined with precision ΔE. Thus, suppose we fix the total energy to be $E_{\text{tot}} = m\Delta E$ with $m \in \mathbb{Z}$, then the projector on this microcanonical subspace is given by

$$P_m = \sum_{x,x'} \delta_{m,x+x'} \Pi_{x,x'}. \tag{13}$$

The Hamiltonian restricted to this subspace is consequently given by

$$H_m \equiv P_m H P_m = \sum_{x,y} \Pi_{x,m-x} H \Pi_{y,m-y}. \tag{14}$$

Specifically, we set (without loss of generality) in the following $E_{\text{tot}} = 0$. Moreover, as sketched in Fig. 2, we consider for simplicity only three participating energy macrostates in A and B, i.e., $P_0 = \Pi_{-1,+1} + \Pi_{0,0} + \Pi_{+1,-1}$. Of course, for a realistic macroscopic system more subspaces should be considered, but three subspaces are sufficient for a proof-of-principle demonstration of our main ideas.

Since the total energy is fixed, we write in the following $(\Pi_-, \Pi_0, \Pi_+) \equiv (\Pi_{-1,+1}, \Pi_{0,0}, \Pi_{+1,-1})$ with associated subspace dimensions (V_-, V_0, V_+). Note that these projectors project on subspaces of systems A and B. The restricted Hamiltonian (14) has consequently nine blocks:

$$H_0 = \begin{pmatrix} H_{--} & H_{-0} & H_{-+} \\ H_{0-} & H_{00} & H_{0+} \\ H_{+-} & H_{+0} & H_{++} \end{pmatrix}. \tag{15}$$

Each of these blocks is in principle fully determined by the microscopic Hamiltonian (12), but we want to capture only four main features here. First, the systems A and B are assumed to be identical from a thermodynamic point of view. In particular, we assume that the relation between energy and temperature is the same in A and B such that their energy difference is proportional to their temperature difference. Second, we consider normal thermodynamic systems where the subspace corresponding to an equal energy distribution (or the same temperature according to the previous agreement) is the largest "equilibrium" subspace, i.e., $V_0 > V_-, V_+$. Third, we assume a weak interaction between A and B; i.e., the interaction energy λH_I is supposed to be negligible (otherwise it would not be justified to restrict the discussion to a microcanonical energy window defined by the sum $E_A + E_B$ of local energies only). Fourth, we want to mimic the interaction of two generic complex (and thus, nonintegrable) many-body systems. According to common knowledge in statistical mechanics, this can be efficiently done by using random matrix theory [59–65].

In unison with these agreements, we consider below the following specific Hamiltonian. The diagonal blocks (H_{--}, H_{00}, H_{++}) are modeled by diagonal matrices with (V_-, V_0, V_+) many equally spaced energies in the interval

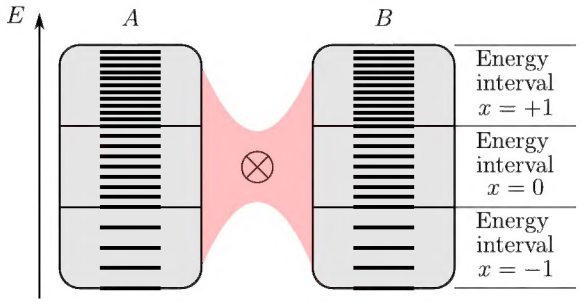

FIG. 2. Sketch of two identical, interacting systems A and B with discrete energy levels. The energies of both A and B are coarse-grained into windows x with an increasing number of levels. Finally, the dynamics is restricted to a microcanonical subspace of the total energy corresponding to windows $(x_A, x_B) = (+1, -1) \cup (0, 0) \cup (-1, +1)$.

$[0, 2\Delta E)$ [88]. Moreover, we set $H_{--} = H_{++}$, implying $V_- = V_+$ such that the total Hilbert space dimension is $D = 2V_- + V_0$. The coupling between different blocks is realized by random matrices $H_{-0} = H_{0-}^\dagger$ and $H_{0+} = H_{+0}^\dagger$ with elements drawn from an orthogonal zero-mean-unit-variance Gaussian ensemble (the unitary Gaussian ensemble is not observed to give rise to different behavior) multiplied by the small coupling constant λ. Note that H_{-0} and H_{0+} are not square matrices since $V_0 > V_-, V_+$. Moreover, in view of the weak interaction, we set $H_{-+} = H_{+-}^\dagger$ to be a matrix of zeros; i.e., we forbid transitions between energy levels that are too far away from each other.

To remain in the regime of weak coupling, but to ensure that the different energy levels in A and B also sufficiently interact to make energy transport efficient, we have to choose λ, ΔE, and the volumes appropriately. Their values can be estimated as follows. First, let us define weak coupling by demanding that the energy of the diagonal part $H_0 = H_{--} + H_{00} + H_{++}$ dominates the interaction energy $\lambda H_I = H_{-0} + H_{0-} + H_{+0} + H_{0+}$. To estimate their typical value, we use an average over the microcanonical ensemble $\langle \ldots \rangle_{\mathrm{mic}}$. For the diagonal part, we find the value $\langle H_0 \rangle_{\mathrm{mic}} \approx \Delta E$. Since $\langle \lambda H_I \rangle_{\mathrm{mic}} = 0$, we look at the standard deviation $\lambda \langle H_I^2 \rangle_{\mathrm{mic}}^{1/2} \approx \lambda \sqrt{V_0 V_\pm / D} \approx \lambda \sqrt{V_\pm}$. Thus, we obtain the condition $\lambda^2 V_\pm / \Delta E^2 \ll 1$ (note that we take λ to have the dimension of energy). To make A and B sufficiently interact, we note that the interaction smears out the local energy eigenstates of A and B proportional to λ ("level broadening"). At the same time, the density of states in the $x = \pm 1$ subspace is roughly $\Delta E / V_\pm$. To guarantee that the smeared-out levels in A (B) overlap with sufficiently many levels in B (A), we thus demand $(\lambda V_\pm / \Delta E)^2 \gg 1$. Specifically, what we found to work numerically well are the conditions

$$\frac{1}{V_\pm}\left(\frac{\pi \lambda V_\pm}{2\Delta E}\right)^2 \ll 1, \qquad 32\left(\frac{\pi \lambda V_\pm}{2\Delta E}\right)^2 \gg 1; \quad (16)$$

compare also with Ref. [89] for an analytical study of a similar model (two equal energy bands coupled via a random matrix). Unless otherwise mentioned, we choose λ below such that the left equation reduces to 0.01 ($\ll 1$), which implies that the right equation is well satisfied for $V_\pm \gtrsim 300$. Moreover, the characteristic evolution timescale has been found to be well approximated by

$$\tau = \frac{\Delta E}{4\pi \lambda^2 V_\pm}. \quad (17)$$

In all that follows, we set $\Delta E = 1$ and $V_0 = 3V_-$.

Finally, we write the initial state as

$$|\psi(t_0)\rangle = \sqrt{p_-(0)}|\psi_-\rangle + \sqrt{p_0(0)}|\psi_0\rangle + \sqrt{p_+(0)}|\psi_+\rangle. \quad (18)$$

Here, $p_x(0)$ with $x \in \{-, 0, +\}$ is the (*a priori* arbitrary) probability to find the system in macrostate x. Unless otherwise mentioned, the states $|\psi_x\rangle$ are normalized Haar randomly chosen states in the subspace $\mathcal{H}_x$ on which Π_x projects. By choosing them Haar randomly, we guarantee an unbiased choice, somewhat in the spirit of a maximum entropy principle for pure states. In particular, given that $p_x(0)$ is the only available information, this allows us to ask about the typical behavior of the system.

B. Results

First, to get a feeling for the average dynamics, we consider the time evolution of the macrostate distribution $p_x(t) = \langle \psi(t)|\Pi_x|\psi(t)\rangle$ in Fig. 3 for two different Hilbert space dimensions. In Fig. 3(a), we start from the nonequilibrium initial condition $[p_-(0), p_0(0), p_+(0)] = (1, 0, 0)$. For $D = 10^4$ (solid lines), we see an exponential (Markovian) decay of the probabilities to their equilibrium value $(V_-, V_0, V_+)/D = (0.2, 0.6, 0.2)$ (thin horizontal black lines) as predicted by statistical mechanics. The characteristic evolution timescale is set by τ, and equilibration happens roughly for $t \gtrsim 7\tau$. For the smaller Hilbert space dimension of $D = 10^2$ (circles), a similar tendency but much larger fluctuations are observed, as expected.

To continue with the many-worlds simulation, we now choose an equilibrium initial state with $p_x(0) = V_x/D$, for reasons that will also become clear later. Naively, one would expect nothing interesting in such a universe as indicated in Fig. 3(b): Aside from fluctuations, which are exponentially suppressed as a function of the Hilbert space dimension, nothing seems to happen. But interestingly, a completely different picture is possible: Even from an equilibrium state, many different interesting nonequilibrium universes can emerge. However, to warrant such a conclusion, we first of all need to ensure that the histories defined by the present coarse-graining are decoherent; i.e., they obey the DHC condition as discussed in the previous section. In the following, the evaluation of the DF is done

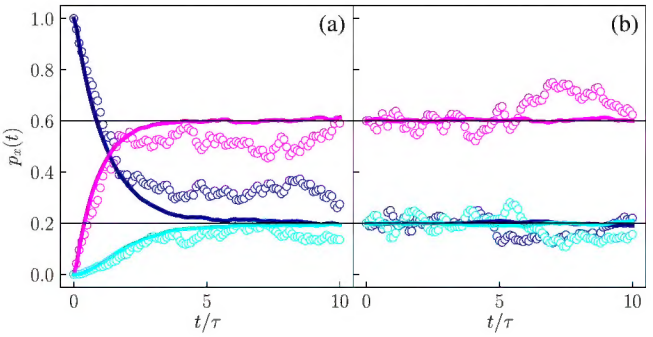

FIG. 3. Time evolution of $p_-(t)$ (dark blue), $p_0(t)$ (magenta), and $p_+(t)$ (cyan) over dimensionless time t/τ for an initial nonequilibrium state (a) or equilibrium state (b) for $D = 10^4$ (solid lines) and $D = 10^2$ (circles). The horizontal black lines indicate the equilibrium value $= (V_-, V_0, V_+)/D$.

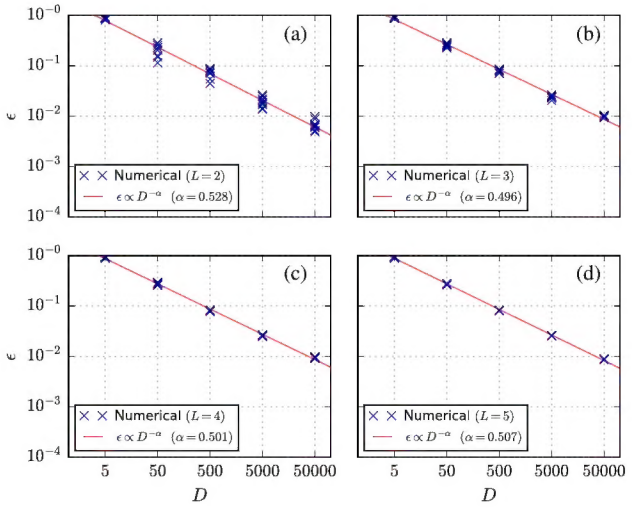

FIG. 4. Plot of ϵ, the average violation of decoherence defined in Eq. (5), in the weak-coupling regime as a function of the Hilbert space dimension for histories of length $L = 2$ (a), $L = 3$ (b), $L = 4$ (c), and $L = 5$ (d). Blue crosses mark results for a single realization of the random matrix interaction and the random initial equilibrium state. Red solid lines fit a scaling law of the form $D^{-\alpha}$ to their averages, and the value of α is indicated in the legend inset. Note the double logarithmic scale.

for constant time intervals $t_{k+1} - t_k$ equal to the nonequilibrium relaxation timescale τ defined in Eq. (17).

The emergence of decoherence is shown in Figs. 4 and 5. First, Fig. 4 plots the average off-diagonal elements of the normalized DF as defined in Eq. (5) for histories of lengths $L \in \{2, 3, 4, 5\}$ as a function of the Hilbert space dimension D. Each marker in Fig. 4 corresponds to one particular random matrix Hamiltonian with one particular Haar random initial equilibrium state defined in Eq. (18). In total, we consider three different realizations of the random matrix Hamiltonian and, for each, three different realizations of the initial state, amounting to $3 \times 3 = 9$ different realizations. To extract the overall trend, we average the markers and fit a scaling law of the form $D^{-\alpha}$ (solid red line).

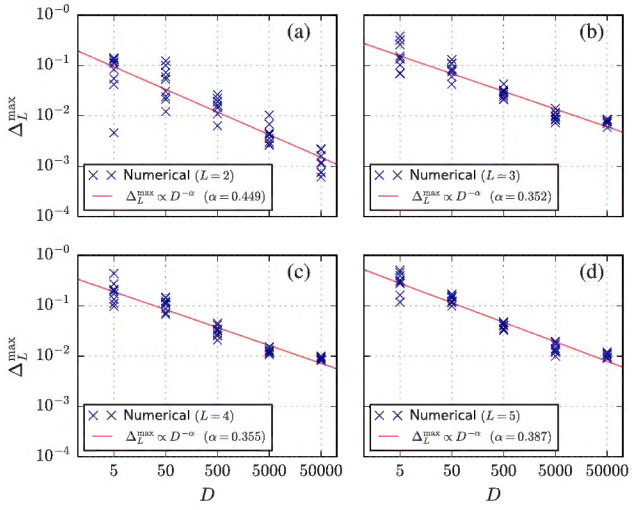

FIG. 5. Plot of $\Delta_L^{\max}$, the worst-case violation of decoherence defined in Eq. (11), with otherwise the same characteristics as in Fig. 4.

Two important observations are contained in Fig. 4. First, the different data points corresponding to different realizations lie very close to each other; i.e., each realization gives rise to a similar value of ϵ. This indicates typicality: Most random matrix interactions and most initial states give rise to the same behavior. Therefore, it makes sense to fit a scaling law $D^{-\alpha}$ to the averaged data points. Interestingly, this scaling law, which we extract by varying D over 4 orders of magnitude from $D = 5$ to $D = 50\,000$, is very close to $1/\sqrt{D}$. This scaling suggests that the conditional states $|\psi(\mathbf{x})\rangle$, after normalization, can be expressed as $\sum_i c_i(\mathbf{x})|i\rangle/\sqrt{D}$ for some fixed basis $|i\rangle$. Here, the $c_i(\mathbf{x})$ are random zero-mean-unit-variance coefficients assumed independent of $c_i(\mathbf{y})$ for $\mathbf{x} \neq \mathbf{y}$ because then a random-walk argument suggests

$$\langle\psi(\mathbf{y})|\psi(\mathbf{x})\rangle \sim \frac{1}{D}\sum_i c_i^*(\mathbf{y})c_i(\mathbf{x}) \sim \frac{1}{\sqrt{D}}. \tag{19}$$

While it seems plausible, it remains an open question whether this inverse square-root dependence holds for all weakly perturbed random matrix theory models and Haar random initial equilibrium states. In any case, the scaling law suggests that quantum effects are exponentially suppressed as a function of the particle number N. Moreover, these conclusions are robust under changing the length $L \in \{2, 3, 4, 5\}$ of the histories. Partial results for very long histories have been also recently obtained by two of the authors [90].

The same conclusions are also reached in Fig. 5, where we plot the maximum value of the trace distance defined in Eq. (11). Also, for this more rigorous quantifier of decoherence, we observe typicality and an exponential suppression of quantum effects as a function of the particle number N. However, since $\Delta_L^{\max}$ is determined by the worst-case scenario, stronger fluctuations are visible compared to ϵ, where the average tames fluctuations. Moreover, the exponent $\alpha \approx 0.4$ is slightly smaller than the exponent extracted in Fig. 4. Nevertheless, Fig. 5 shows that also statistical outliers, which could be potentially detected by a clever and patient experimentalist, do not corrupt our conclusions. We conclude that the emergence of decoherence seems to be a stable and robust phenomenon.

It is intriguing to ask whether histories or branches that look more distinct from a macroscopic point of view are characterized by stronger decoherence. Specifically, let us define the Hamming distance $d(\mathbf{x}, \mathbf{y})$ between two histories $\mathbf{x}$ and $\mathbf{y}$ as the number of labels where they differ. For instance, for $\mathbf{x} = (0, +, 0, -, 0)$ and $\mathbf{y} = (0, -, +, 0, 0)$

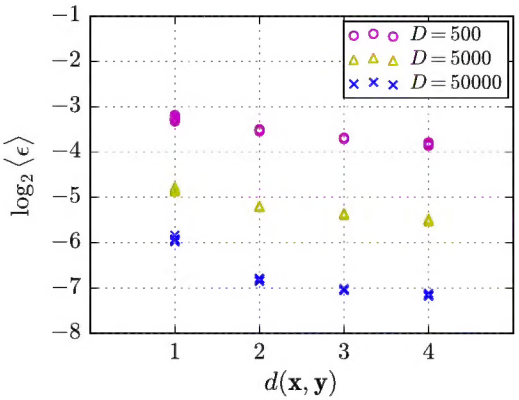

FIG. 6. Average decoherence $\langle\epsilon\rangle$ as a function of the history distance $d(\mathbf{x},\mathbf{y})$. Here, $\langle\epsilon\rangle = \sum_{d'=d(\mathbf{x},\mathbf{y})} \epsilon(\mathbf{x};\mathbf{y})/\#(d')$ sums the normalized DF in Eq. (4) over all pairs of histories with a fixed distance $d' = d(\mathbf{x},\mathbf{y})$ divided by the number $\#(d')$ of such pairs. We display results for $D = 500$ (magenta circles), $D = 5000$ (yellow triangles), and $D = 50\,000$ (blue crosses) for $L = 5$ and for the same nine realizations as in Figs. 4 and 5.

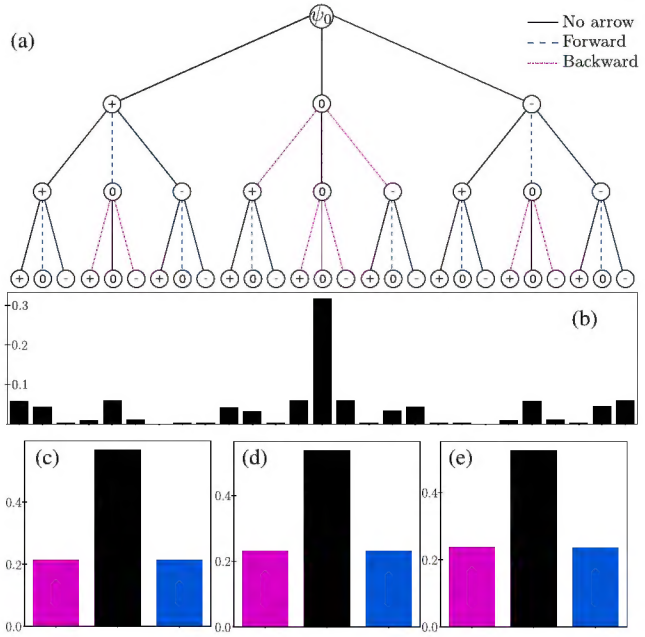

FIG. 7. (a) Depiction of the branching structure of the multiverse with respect to the initial time t_0 and with respect to our chosen coarse-graining. (b) Histogram for the probabilities of different histories. For $L = 3$ (c), $L = 4$ (d), and $L = 5$ (e), respectively, we plot the probability of universes with different (net) arrows of time as explained in the main text. All probabilities are obtained for a single realization of the interaction Hamiltonian (at weak coupling and for $D = 10000$) and initial equilibrium state.

we have $d(\mathbf{x},\mathbf{y}) = 3$. Even though, to the best of our knowledge, this question has never been asked before, it seems intuitive to expect that more distinct histories show stronger decoherence. This intuition is indeed confirmed in Fig. 6, even though the dependence on the distance $d(\mathbf{x},\mathbf{y})$ is rather mild: an approximate twofold increase in decoherence when going from $d(\mathbf{x},\mathbf{y}) = 1$ to $d(\mathbf{x},\mathbf{y}) = 4$. However, in more realistic scenarios one would need to take into account much longer histories. Moreover, it seems that the differences are more pronounced for larger Hilbert space dimensions D. Unfortunately, current numerical limitations do not allow us to draw strong conclusions from our data.

The overall picture that emerges from our model is depicted in Fig. 7. Figure 7(a) shows a branching tree structure with respect to histories defined by energetic macrostates labeled by $x \in \{-, 0, +\}$ for $L = 3$ time steps. Importantly, we can now reason about these histories using a classical ontological model for sufficiently large D. To facilitate talking about it, we use Boltzmann's entropy concept $S_B(x) = k_B \ln V_x$. We label transitions of the system from a lower to a higher Boltzmann entropy state (i.e., from $+$ or $-$ to 0) as "forward" transitions (blue dashed lines) to indicate that they comply with the conventional second lawlike arrow of time when t_0 denotes the initial time. However, "backward" transitions (pink dash-dotted lines) from a higher- to a lower-entropy state (i.e., from 0 to $+$ or $-$) are also possible. Finally, transitions involving no change in Boltzmann entropy are labeled by "no arrow" (black lines). The multiverse thus consists of different histories or branches that do not interfere and that describe universes with different entropic arrows of time (including the possibility of universes with no arrow of time and both arrows of time) determined by the question whether heat flows from hot to cold or vice versa. Note that these entropic arrows of time should be distinguished from the "branching arrow of time" (i.e., the direction in which the number of branches increases). The branching arrow is pure convention and unrelated to the perceived entropic arrow of time within the universes.

For one realization of the Hamiltonian and one realization of the initial state, we depict the probability for each history, which can be now interpreted classically, by the histogram below the treelike branching structure in Fig. 7(b). As a consistency check, we immediately see that the history $\mathbf{x} = (0, 0, 0)$, in which the Universe resides in the dominant equilibrium macrostate $x = 0$, is the most probable one. Note that the probability for this history is different from the probability $(V_0/D)^3 = 0.6^3 = 0.216$ that one would expect by sampling the histories at time intervals comparable to the equilibration time. The time steps τ we use are clearly in the nonequilibrium regime.

An important consistency check is to ask about the probability of forward or backward arrows of time. Since the Schrödinger equation obeys time-reversal symmetry and since the initial equilibrium state that we chose also does not introduce any time asymmetry, we should expect to get a time-symmetric answer in this case. The answer is shown in Figs. 7(c)–7(e) where we plot the probability for a forward arrow of time (blue), no arrow of time (black), and

a backward arrow of time (pink) for histories of length $L = 3$, $L = 4$, and $L = 5$, respectively. Here, histories with multiple arrows of time contribute according to their "net" arrow of time; i.e., the history $\mathbf{x} = (0, +, 0)$ has no overall arrow of time. Owing to the fact that we have only three macrostates, there can be no histories with two or more net forward or backward arrows of time. Thus, our model exhibits only "mini" entropic arrows of time, unable to account for our arrow of time in reality. Clearly, by including more than three energy windows in the coarse-graining, we could observe longer arrows of time in this model, but their probability (when starting from an equilibrium state) would be very small, albeit nonzero. This is the (in)famous Boltzmann brain paradox [91–93]. In any case, we see that the arrows are indeed symmetrically distributed in our model as they should be. Some nonvisible small random fluctuations (in the third significant digit) are due to the fact that a random initial state can still have a small preference to evolve into a higher- or lower-entropy region; i.e., it is not perfectly symmetric under time reversal. The histograms in Fig. 7 are based on a single realization of the Hamiltonian and initial state, but we again found this behavior to be typical.

We continue by challenging our model. This is first done by considering an atypical initial state in the form of a randomly selected energy eigenstate $|k\rangle$ of the full Hamiltonian. From the eigenstate thermalization hypothesis [64,65,94–97], it is known that these states give rise to probabilities $p_x = \langle k|\Pi_x|k\rangle$ very close to the thermal (microcanonical) prediction V_x/D, i.e., a picture similar to Fig. 3(b). However, it is currently not known whether multitime correlation functions such as the DF display the same behavior for energy eigenstates and Haar randomly sampled equilibrium states.

The results for the emergence of decoherence with initial energy eigenstates are shown in Figs. 8 and 9. We again observe a rather typical behavior in Fig. 8 and a scaling law suggesting the exponential suppression of quantum effects as a function of the particle number. However, compared with Figs. 4 and 5, the variance in the data points is appreciably larger; i.e., there is less typicality. Moreover, the exponents are different. For ϵ we find $\alpha \approx 0.44$, which is close to the previous value of $\alpha \approx 0.5$. Instead, for $\Delta_L^{\max}$ we find $\alpha \approx 0.2$, which is half the value we found for Haar random initial equilibrium states. Moreover, $\Delta_L^{\max}$ fluctuates strongly for different realizations such that the fitted scaling law (red solid line) provides only a rough orientation. Thus, the preliminary conclusions that we can draw from these data is that correlation functions of energy eigenstates behave differently from Haar random equilibrium states (which will typically overlap with many energy eigenstates), which is an interesting result in its own right. In particular, Albrecht *et al.* recently introduced an "eigenstate einselection hypothesis" (Appendix B in Ref. [39]), where they claim that the "general features of the consistent histories quantities are unchanged" for energy eigenstates. On a quantitative level, we see here clear evidence for the opposite, but from a qualitative point of view we observe the same: The difference between $D^{-0.4}$ and $D^{-0.2}$ might not matter in practice, say, for $D \geq 10^{100}$. Thus, the emergence of decoherence as studied here seems to be a rather robust phenomenon if we restrict the attention to slow and coarse observables of a nonintegrable quantum many-body system.

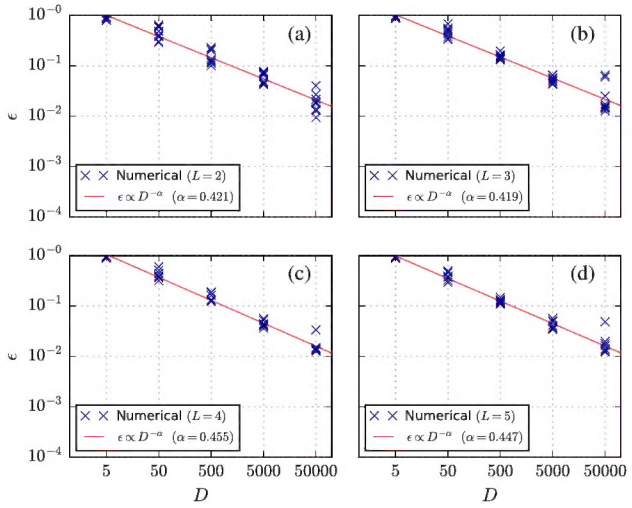

FIG. 8. Plot of ϵ for a random initial energy eigenstate. Blue crosses refer to three different randomly chosen eigenstates repeated for three different realizations of the random matrix coupling, i.e., nine realizations in total. Other details are as in Fig. 4.

We remark that we have also studied the case of perturbed projectors of the form $V_\delta \Pi_x V_\delta^\dagger$, where the unitary $V_\delta = e^{iA\delta}$ rotates the projectors using a Hermitian matrix $A = A^\dagger$. However, for various A's we found quantitatively

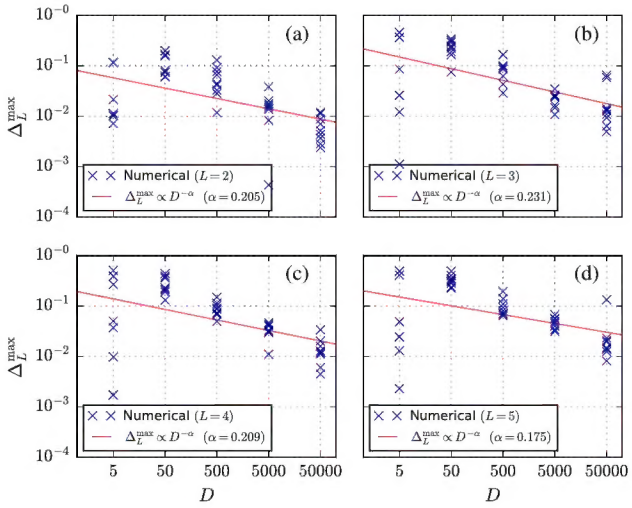

FIG. 9. Plot of $\Delta_L^{\max}$ with otherwise the same characteristics as in Fig. 8.

similar results (apart from fluctuations). [We checked three cases: $A_{ij} = \delta_{i\pm1,j}$ and $A_{ij} = \delta_{i+j,D+1}$ (with respect to the eigenbasis of the unperturbed Hamiltonian) and A randomly drawn according to the same distribution as H_I.] Therefore, and also to keep the manuscript concise, we do not display these results here, but we believe a systematic study is an interesting task for the future.

Instead, we find it important to illustrate that the emergence of decoherence is not a universal phenomenon valid for all observables. To demonstrate this, we consider the case of two strongly coupled systems exchanging energy. To this end, we increase λ to 10λ such that the right-hand side of the first equation in Eq. (16) equals 1. Because of the strong interaction, local energy exchanges will now happen quickly. In some sense, it is no longer meaningful to talk about the local energies of A and B since the local energy levels of systems A and B will strongly hybridize to form new levels.

While the considered observable has the same coarseness, we now observe a quite different behavior of decoherence in Figs. 10 and 11. While typicality still holds well, a much milder exponential suppression of quantum effects is observed for ϵ and histories of length $L \geq 3$, with a scaling exponent around $\alpha = 0.15$ (Fig. 10). Even more drastic changes appear for $\Delta_L^{\max}$ (Fig. 11) with an exponent $\alpha \approx 0$ for $L = 5$ (indicating perhaps a power-law suppression or no suppression at all). Recalling that we have to base our conclusions on a finite (and rather small) amount of samples, a clear-cut conclusion does not seem possible: Exponential suppression of quantum effects, which requires $\alpha > 0$, seems possible but is not warranted, and it is certainly much weaker than in the weak-coupling (slow observable) regime.

Notably, exponential suppression of quantum effects (with a large exponent $\alpha \approx 0.5$) still holds for the shortest

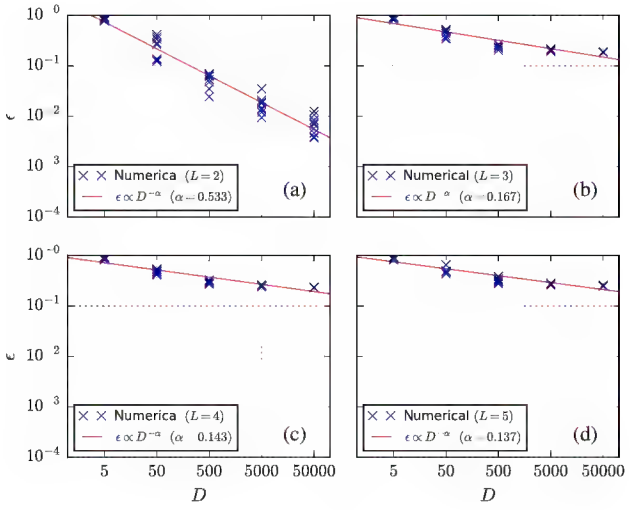

FIG. 10. Plot of ϵ at strong coupling with otherwise the same characteristics as in Fig. 4.

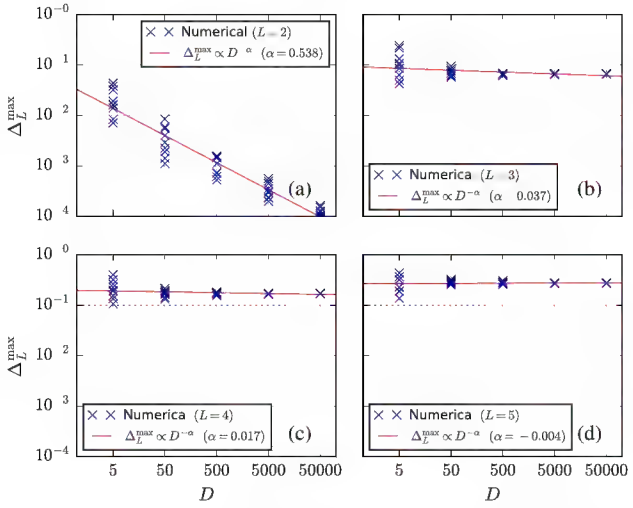

FIG. 11. Plot of $\Delta_L^{\max}$ at strong coupling with otherwise the same characteristics as in Fig. 5.

length of histories with $L = 2$. This seems counterintuitive, but it can be explained by recalling that we have chosen a Haar random initial equilibrium state of the form (18) with $p_x(0) = V_x/D$ in Figs. 10 and 11. The two-time DF then probes only quantum features of a two-time equilibrium correlation function. They are decoherent because, first, $\mathbb{E}[\Pi_{x_0}|\psi(t_0)\rangle\langle\psi(t_0)|\Pi_{y_0}] \sim \delta_{x_0,y_0}$ where $\mathbb{E}[\ldots]$ denotes a Haar random average, and second, typicality implies that most pure states $|\psi(t_0)\rangle$ behave similarly. Indeed, for this situation an analytical proof of decoherence has been given in Ref. [49].

We end this central part of the manuscript by pointing out that we have tested the robustness of our conclusions in various further situations for an initial Haar random equilibrium state. For instance, we considered random time spacings $t_{k+1} - t_k$ chosen uniformly either from $[0, \tau]$ or $[\tau, 2\tau]$ (instead of the constant time spacing of $t_{k+1} - t_k = \tau$ considered here), we considered random instead of equally spaced energies in the diagonal Hamiltonian blocks of Eq. (15), we used the Gaussian unitary ensemble instead of the Gaussian orthogonal ensemble for the off-diagonal blocks of Eq. (15), and we also plotted other quantifiers that one could derive from the DHC (3). In all these cases, we observed the same qualitative behavior, i.e., the typicality of a decay law of the form $D^{-\alpha}$. We do not show these results here to keep the manuscript at a reasonable length.

IV. SET SELECTION PROBLEM

The set selection problem has been used to criticize the histories formalism by pointing out that the DHC is incomplete [18,22–25,27,30,98]. The basic reasoning behind the criticism is the following. Consider for fixed L and M the manifold $\mathtt{H}$ of all possible projectors that can be used to define histories $\mathbf{x}$ (of very different physical meaning). The dimension of this manifold scales like D^{2L},

whereas the number of constraints imposed by the DHC in Eq. (3) scales like M^{2L}. Thus, the submanifold DH of decoherent histories has a dimension that scales like $D^{2L} - M^{2L}$, which (even though of measure zero with respect to H) is enormous for $D \gg M$. Hence, which of the many physically very distinct histories should one use? Note the close similarity to the preferred basis problem.

Here we discuss the set selection problem based on the robust numerical findings from above (for further discussion, see also Ref. [21]). In particular, and contrary to previous claims, we suggest that there simply is no set selection problem if one focuses on slow and coarse observables of many-body systems—that is, situations relevant to human perception—and the remaining freedom in the choice of observable is actually important for the ability of different observers to agree.

The key to our argument is to demand a certain stability or robustness of decoherence with respect to the initial state $|\psi(t_0)\rangle$ and times t_k and to focus on approximate instead of exact decoherence, which is sufficient for all practical purposes. To recall our results above: We found approximate decoherence without exception for slow and coarse observables for a large set of initial states, times, and Hamiltonians. In contrast, it seems likely that the vast majority of decoherent histories in DH is not robust in this sense. Instead, it likely depends sensitively on, e.g., $|\psi(t_0)\rangle$, as sketched in Fig. 12.

For instance, one example is a coarse-graining $\{\Pi_x(t_k)\}$ at time t_k with one projector, say, the first for $x = 1$, equal to $\Pi_1(t_k) = |\psi(t_k)\rangle\langle\psi(t_k)|$. Here, $|\psi(t_k)\rangle = U_{k,0}|\psi(t_0)\rangle$ is the unitarily evolved initial state. This coarse-graining satisfies by construction the DHC, but it is very sensitive to $\psi(t_0)$ and t_k: Changing them while leaving the projectors fixed will quickly destroy decoherence.

One might object that those examples are nevertheless legitimate, but there are fundamental practical obstacles. First, it is unclear how humans should get access to a projector of the form $|\psi(t_k)\rangle\langle\psi(t_k)|$ using earthly instruments. Second, if the MWI is correct, then knowledge of the global $|\psi(t_k)\rangle$ is impossible since observers are limited to their own branch $|\psi(\mathbf{x})\rangle$. Finally, proper relativistic considerations teach us that at any given time t we can access only part of the universal wave function $\rho_{\text{accessible}}(t) = \text{tr}_{\text{inaccesible}}\{|\psi(t)\rangle\langle\psi(t)|\}$. Thus, even if we assume we find (by some magic instrument) a strange decoherent history depending on $\rho_{\text{accessible}}(t)$, decoherence would likely be destroyed in the next second once a new photon from a hitherto unobserved star reaches us.

Admittedly, this is not a rigorous argument showing that most of the histories in DH are of this fragile nature, but one should also admit in defense of this argument that an interesting example of stable and robust decoherent histories (beyond what we discussed here) has never been presented. Thus, we conjecture that the set selection problem is solvable by focusing on locally and practically accessible, approximately decoherent histories that are stable and robust.

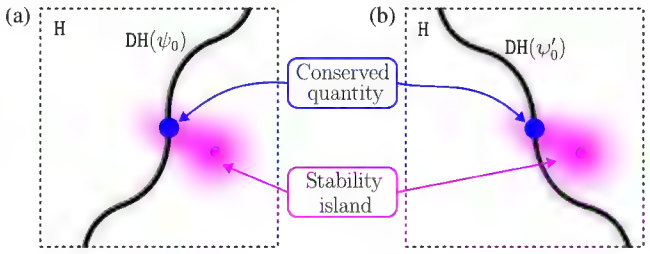

FIG. 12. The square depicts the manifold H of all histories, and the shade indicates the amount of decoherence (white regions correspond to no decoherence). The dark black line depicts the submanifold DH of exactly decoherent histories, which is very sensitive to different initial states $\psi(t_0)$ (a) and $\psi'(t_0)$ (b). All DH(ψ_0) intersect for histories of conserved quantities (blue dot, exaggerated in size). Most important to our argument is the stability island (pink shaded region) of approximately decoherent histories, which remains (almost) unchanged for (a) and (b).

We further strengthen the argument by pointing out the similarity with debates dating back to Boltzmann, Loschmidt, and Zermelo. For a given initial state, it is possible to find a continuum of observables that does not thermalize or entropies that violate the second law, a fact well known in pure state statistical mechanics. But all these artificially constructed counterexamples are of little relevance because the smallest perturbation of the initial state or Hamiltonian causes them to behave in agreement with thermodynamics again.

In addition, we believe that approximate (instead of exact) decoherence is key to resolve this problem because approximate decoherence can be very robust; see the "stability island" in Fig. 12. (In addition, our scaling law indicates for realistic many-body systems that approximate decoherence becomes practically indistinguishable from exact decoherence.) Indeed, two different observers never perceive exactly the same observable (for instance, by reading of a display at slightly different angles), but both should still have compatible perceptions (this point is also central to quantum Darwinism [28–30]). Thus, instead of trying to find a single spot in the history space H that is exactly decoherent, it is more important to find the extended region that guarantees robust approximate decoherence. In this respect, we are sceptical about the idea that approximately decoherent histories can be always slightly distorted to become exactly decoherent [18,23,83,99]: Not only is it unclear how to define a slight distortion, but it also seems unlikely that this distortion will be robust (independent of ψ_0 and t_k).

Thus, the picture that emerges is that of a robust stability island that describes accessible and almost exactly decoherent histories for large systems. This stability island is itself a huge region but for good reasons. First, it guarantees that different observers can have similar perceptions of

classical reality. Second, the set of slow observables in this stability island will approximately commute for large systems, thus allowing one to define joint decoherent histories describing, e.g., the position, momentum, and energy of a flying stone. (However, the technical details of how to precisely handle approximately commuting observables are still subject to research [100–102].)

We finish with two remarks. First, there is also an unappreciated set selection problem in EID. Gauge symmetries imply that there is a continuum of physically equivalent system-environment tensor product splittings of the same physical system [103,104]. Each splitting gives rise to a different system-environment Hamiltonian and, consequently, a different pointer basis. Of course, what matters in practice is that the pointer basis is compatible with the experimental measurement procedure, but this resolution of the "pointer basis selection problem" is identical in spirit to the resolution proposed here in the histories context.

Second, we repeat that the proposed solution is restricted to slow and coarse observables of many-body systems that approximately decohere. It does not solve the set selection problem if one demands exact decoherence. Also, other fundamental problems within the histories formalism such as the one debated in Refs. [105–107] are not directly influenced by our argument.

V. CONCLUDING PERSPECTIVES

A. Summary

We presented a direct evaluation of the DF for multiple (up to five) time steps from first principles for a nontrivial example. We rigorously defined quantum-interference effects and extracted a scaling law of the form $D^{-\alpha}$ by varying the Hilbert space dimension D over 4 orders of magnitude. This was checked for a wide variety of situations, and it provided a firm starting point to quantitatively discuss the DHC.

The resulting picture is that coarse and slow observables of nonintegrable many-body systems give rise to a robust and stable form of approximate decoherence. While our calculations were restricted to a particular model, the success and versatility of random matrix theory suggests that our results are more widely applicable; see also Refs. [39,41,49,50,66–68] for supporting evidence.

Based on this evidence, we suggested that the preferred basis problem of the MWI or the set selection problem of the histories formalism, respectively, is solvable if one is interested in observables relevant to us humans (which are slow and coarse and give rise to a robust and stable form of decoherence) and if one focuses on approximate instead of exact decoherence. Indeed, our results indicated that for such observables the emergence of decoherence is universal and happens for almost all pure states: No product state assumption, no low-entropy initial state, and no ensemble average were necessary in our approach. Moreover, it seems reasonable to expect (but difficult to prove) that possible ambiguities in the choice of branches and histories become irrelevant as different slow and coarse obervables approximately commute for large quantum systems.

Importantly, this picture does not contradict previous works, but it complements and extends them by providing new perspectives, tools, and insights. For instance, our results do not rely on the widely used concepts of EID and quantum Darwinsim, but they are not in conflict with them. Indeed, a $1/\sqrt{D}$ scaling law has been also extracted for a random matrix model in the context of EID [108]. Moreover, we believe nonintegrability is a key factor, but it is usually not regarded as such in other works on the quantum-to-classical transition.

Finally, we also explicitly saw that an equilibrated multiverse gives rise to branches with locally well-defined entropic arrows of time, while overall, the multiverse remains statistically time symmetric. While our model could be claimed to be unrealistic because of the Boltzmann brain paradox [91–93], it nevertheless explicitly illustrates two crucial features. First, the branching structure of the multiverse is pure convention and does not explain our arrow of time or meaningful thermodynamic entropy, contrary to suggestions made in Refs. [109,110]. Instead, from a fundamental point of view it would be preferable to start from a time-symmetric description of the MWI or histories formalism [19,111–114]. Second, opposite arrows of time can peacefully coexist within the same quantum multiverse, in contrast to opposite arrows of time in spacelike separated regions of a classical multiverse [115], which are unstable with respect to the slightest perturbation [116]. For further details about the emergence of classicality in time-symmetric situations, see Ref. [39]. Moreover, that arrows of time can be an emergent concept in a time-reversal symmetric universe was also noted in different contexts, e.g., in Refs. [115,117–119].

B. Outlook

Our work could stimulate various research directions, as it combines tools and concepts related to the quantum-to-classical transition, quantum cosmology, quantum statistical mechanics, and quantum stochastic processes.

For instance, while we argued that nonintegrability could be a key factor, chaos has been also realized as detrimental for the emergence of classicality within the Wheeler-DeWitt equation due to the breakdown of the WKB approximation, and EID was invoked to remedy for that [120–122]. Within our nonrelativistic quantum-mechanical model, we cannot make any direct contribution to this question, but one view suggested by this work is that emergence of classicality is best viewed as a synergy of different mechanisms instead of a single all-ruling idea.

Indeed, it has been recently pointed out that the emergence of classicality in the early Universe is still an unsolved puzzle [123], and the present perspective might be able to add a piece to it.

Moreover, it would be desirable to get a better analytical understanding of the DHC. The results reported in Refs. [41,49] were restricted to three-time correlation functions and generalizing them to higher orders likely requires novel techniques (however, some progress for arbitrary L-time correlation functions in a different context was reported in Refs. [47,48,124,125]). Further insights into the timescales at which decoherence arises are also desirable, and it is in particular also worth asking about "recoherence times": Because of Poincaré recurrences, the emergence of decoherence in a finite-dimensional quantum system cannot be a persistent, eternal phenomenon. In particular, it would be intriguing to find out how the recoherence time scales with the number of time steps L or, more generally, with the net information acquired along a history. In addition, it seems that more research is necessary to understand the general consequences of approximate instead of exact decoherence given that the latter is not the rule.

We further remark that we used the conventional framework of nonrelativistic quantum mechanics and assumed the validity of the Born rule. A significant fraction of research is devoted to interpreting or understanding the origin of the Born rule within the MWI (see, e.g., Refs. [5,6,30,36,126,127] and references therein). The present approach could also add insights into this debate when considering very long histories for $L \gg 1$, as recently studied by two of the authors [90].

Finally, our model calculations presently suggest that for any coarse and slow observable of a nonintegrable system, every possible classical history is realized. While this suggests the realization of a wide array of histories, it is not necessarily true that "everything that can happen will happen" (as sometimes portrayed in both scientific and popular accounts of the MWI). For instance, extremely unlikely (sequences of) outcomes might be restricted to very small subspaces because they are highly atypical, but our results indicated that large subspaces are needed for the emergence of classicality; see also Ref. [90]. We also collected some evidence in Fig. 6 that there is structure in the multiverse among different branches, but much more work in that direction needs to be done. Finally, whether all the perceived randomness in our world stems from quantum effects [128] or not [129] remains a fascinating question, too.

Note added. Recently, evidence appeared that confirms our results for realistic quantum-chaotic many-body systems and suggests that integrable finite-size systems show a much weaker form of decoherence [130].

ACKNOWLEDGMENTS

We are grateful to Anthony Aguirre, Josh Deutsch, Jonathan Halliwell, and Anastasiia Tiutiakina for discussions. P. S. is financially supported by "la Caixa" Foundation (ID No. 100010434, Fellowship No. LCF/BQ/PR21/11840014) and acknowledges further support from the European Commission QuantERA grant ExTRaQT (Spanish MICINN Project No. PCI2022-132965), by the Spanish MINECO (Project No. PID2019–107609 GB-I00) with the support of FEDER funds, the Generalitat de Catalunya (Project No. 2017-SGR-1127), and by the Spanish MCIN with funding from European Union NextGenerationEU (PRTR-C17.I1). J. S. acknowledges support by MICIIN with funding from European Union NextGenerationEU (PRTR-C17.I1) and by the Generalitat de Catalunya.

[1] H. Everett, *"Relative state" formulation of quantum mechanics*, Rev. Mod. Phys. **29**, 454 (1957).
[2] B. S. De Witt, *Quantum mechanics and reality*, Phys. Today **23**, No. 9, 30 (1970).
[3] L. Vaidman, Stanford Encyclopedia of Philosophy (2021), https://plato.stanford.edu/entries/qm-manyworlds/.
[4] *Universe or Multiverse?*, edited by B. Carr (Cambridge University Press, Cambridge, England, 2007).
[5] *Many Worlds? Everett, Quantum Theory, and Reality*, edited by S. Saunders, J. Barrett, A. Kent, and D. Wallace (Oxford University Press, Oxford, 2010).
[6] D. Wallace, *The Emergent Multiverse: Quantum Theory According to the Everett Interpretation* (Oxford University Press, Oxford, 2012).
[7] S. Carroll, *Solo: The philosophy of the multiverse*, https://www.preposterousuniverse.com.
[8] *Everything Everywhere All at Once*, directed by D. Kwan and D. Scheinert (2022), https://en.wikipedia.org/wiki/Everything_Everywhere_All_at_Once.
[9] N. Gisin, *The multiverse pandemic*, arXiv:2210.05377.
[10] M. Tegmark, *Parallel universes*, Sci. Am. **288**, 40 (2003).
[11] K. Barad, *Meeting the Universe Halfway: Quantum Physics and the Entanglement of Matter and Meaning* (Duke University Press, Durham, 2007).
[12] R. B. Griffiths, *Consistent histories and the interpretation of quantum mechanics*, J. Stat. Phys. **36**, 219 (1984).
[13] M. Gell-Mann and J. B. Hartle, *Complexity, Entropy and the Physics of Information* (Addison-Wesley, Reading, MA, 1990), ch. 28, pp. 425–459.
[14] R. Omnès, *Consistent interpretations of quantum mechanics*, Rev. Mod. Phys. **64**, 339 (1992).
[15] H. F. Dowker and J. J. Halliwell, *Quantum mechanics of history: The decoherence functional in quantum mechanics*, Phys. Rev. D **46**, 1580 (1992).
[16] M. Gell-Mann and J. B. Hartle, *Classical equations for quantum systems*, Phys. Rev. D **47**, 3345 (1993).
[17] J. J. Halliwell, *A review of the decoherent histories approach to quantum mechanics*, Ann. N.Y. Acad. Sci. **755**, 726 (1995).

[18] F. Dowker and A. Kent, *On the consistent histories approach to quantum mechanics*, J. Stat. Phys. **82**, 1575 (1996).

[19] R. B. Griffiths, *Consistent Quantum Theory* (Cambridge University Press, Cambridge, England, 2002).

[20] M. Gell-Mann and J. B. Hartle, *Quasiclassical coarse graining and thermodynamic entropy*, Phys. Rev. A **76**, 022104 (2007).

[21] R. B. Griffiths, Stanford Encyclopedia of Philosophy (2019), https://plato.stanford.edu/entries/qm-consistent-histories/.

[22] J. P. Paz and W. H. Zurek, *Environment-induced decoherence, classicality, and consistency of quantum histories*, Phys. Rev. D **48**, 2728 (1993).

[23] F. Dowker and A. Kent, *Properties of consistent histories*, Phys. Rev. Lett. **75**, 3038 (1995).

[24] C. J. Riedel, W. H. Zurek, and M. Zwolak, *Objective past of a quantum universe: Redundant records of consistent histories*, Phys. Rev. A **93**, 032126 (2016).

[25] W. H. Zurek, *Decoherence, einselection, and the quantum origins of the classical*, Rev. Mod. Phys. **75**, 715 (2003).

[26] E. Joos, H. D. Zeh, C. Kiefer, D. Giulini, J. Kupsch, and I.-O. Stamatescu, *Decoherence and the Appearance of a Classical World in Quantum Theory* (Springer, Berlin, 2003).

[27] M. Schlosshauer, *Quantum decoherence*, Phys. Rep. **831**, 1 (2019).

[28] W. H. Zurek, *Quantum Darwinism*, Nat. Phys. **5**, 181 (2009).

[29] J. K. Korbicz, *Roads to objectivity: Quantum Darwinism, spectrum broadcast structures, and strong quantum Darwinism—a review*, Quantum **5**, 571 (2021).

[30] W. H. Zurek, *Quantum theory of the classical: Einselection, envariance, quantum Darwinism and extantons*, Entropy **24**, 1520 (2022).

[31] J. Finkelstein, *Definition of decoherence*, Phys. Rev. D **47**, 5430 (1993).

[32] S. Saunders, *Decoherence, relative states, and evolutionary adaptation*, Found. Phys. **23**, 1553 (1993).

[33] L. Diósi, N Gisin, J. Halliwell, and I. C. Percival, *Decoherent histories and quantum state diffusion*, Phys. Rev. Lett. **74**, 203 (1995).

[34] T. A. Brun, *Quantum jumps as decoherent histories*, Phys. Rev. Lett. **78**, 1833 (1997).

[35] T. Yu, *Decoherence and localization in quantum two-level systems*, Physica (Amsterdam) **248A**, 393 (1998).

[36] L. Vaidman, *On schizophrenic experiences of the neutron or why we should believe in the many-worlds interpretation of quantum theory*, Int. Stud. Philos. Sci. **12**, 245 (1998).

[37] T. A. Brun, *Continuous measurements, quantum trajectories, and decoherent histories*, Phys. Rev. A **61**, 042107 (2000).

[38] C. J. Riedel, *Classical branch structure from spatial redundancy in a many-body wave function*, Phys. Rev. Lett. **118**, 120402 (2017).

[39] A. Albrecht, R. Baunach, and A. Arrasmith, *Einselection, equilibrium, and cosmology*, Phys. Rev. D **106**, 123507 (2022).

[40] A. Touil, F. Anza, S. Deffner, and J. P. Crutchfield, *Branching states as the emergent structure of a quantum universe*, arXiv:2208.05497.

[41] P. Strasberg, *Classicality with(out) decoherence: Concepts, relation to Markovianity, and a random matrix theory approach*, SciPost Phys. **15**, 024 (2023).

[42] F. A. Pollock, C. Rodríguez-Rosario, T. Frauenheim, M. Paternostro, and K. Modi, *Operational Markov condition for quantum processes*, Phys. Rev. Lett. **120**, 040405 (2018).

[43] L. Li, M. J. W. Hall, and H. M. Wiseman, *Concepts of quantum non-Markovianity: A hierarchy*, Phys. Rep. **759**, 1 (2018).

[44] S. Milz and K. Modi, *Quantum stochastic processes and quantum non-Markovian phenomena*, PRX Quantum **2**, 030201 (2021).

[45] R. Dümcke, *Convergence of multitime correlation functions in the weak and singular coupling limits*, J. Math. Phys. (N.Y.) **24**, 311 (1983).

[46] G. W. Ford and R. F. O'Connell, *There is no quantum regression theorem*, Phys. Rev. Lett. **77**, 798 (1996).

[47] P. Figueroa-Romero, K. Modi, and F. A. Pollock, *Almost Markovian processes from closed dynamics*, Quantum **3**, 136 (2019).

[48] P. Figueroa-Romero, F. A. Pollock, and K. Modi, *Markovianization with approximate unitary designs*, Commun. Phys. **4**, 127 (2021).

[49] P. Strasberg, A. Winter, J. Gemmer, and J. Wang, *Classicality, Markovianity, and local detailed balance from pure-state dynamics*, Phys. Rev. A **108**, 012225 (2023).

[50] N. Van Kampen, *Quantum statistics of irreversible processes*, Physica **20**, 603 (1954).

[51] T. A. Brun and J. J. Halliwell, *Decoherence of hydrodynamic histories: A simple spin model*, Phys. Rev. D **54**, 2899 (1996).

[52] J. J. Halliwell, *Decoherent histories and hydrodynamic equations*, Phys. Rev. D **58**, 105015 (1998).

[53] J. J. Halliwell, *Decoherent histories and the emergent classicality of local densities*, Phys. Rev. Lett. **83**, 2481 (1999).

[54] E. A. Calzetta and B. L. Hu, *Influence action and decoherence of hydrodynamic modes*, Phys. Rev. D **59**, 065018 (1999).

[55] J. J. Halliwell, *Decoherence of histories and hydrodynamic equations for a linear oscillator chain*, Phys. Rev. D **68**, 025018 (2003).

[56] J. Halliwell, *Many Worlds? Everett, Quantum Theory, and Reality* (Oxford University Press, Oxford, 2010), ch. 3, pp. 99–118.

[57] N. G. van Kampen, B. DeWitt, S. Goldstein, J. Bricmont, R. B. Griffiths, and R. Omnès, *Quantum histories, mysteries, and measurements*, Phys. Today **53**, No. 5, 76 (2000).

[58] N. G. van Kampen, *The scandal of quantum mechanics*, Am. J. Phys. **76**, 989 (2008).

[59] E. Wigner, *Random matrices in physics*, SIAM Rev. **9**, 1 (1967).

[60] T. A. Brody, J. Flores, J. B. French, P. A. Mello, A. Pandey, and S. S. M. Wong, *Random-matrix physics: Spectrum and strength fluctuations*, Rev. Mod. Phys. **53**, 385 (1981).

[61] C. W. J. Beenakker, *Random-matrix theory of quantum transport*, Rev. Mod. Phys. **69**, 731 (1997).

[62] T. Guhr, Müller-Groeling A, and H. A. Weidenmüller, *Random-matrix theories in quantum physics: Common concepts*, Phys. Rep. **299**, 189 (1998).
[63] F. Haake, *Quantum Signatures of Chaos* (Springer-Verlag, Berlin, 2010).
[64] L. D'Alessio, Y. Kafri, A. Polkovnikov, and M. Rigol, *From quantum chaos and eigenstate thermalization to statistical mechanics and thermodynamics*, Adv. Phys. **65**, 239 (2016).
[65] J. M. Deutsch, *Eigenstate thermalization hypothesis*, Rep. Prog. Phys. **81**, 082001 (2018).
[66] J. Gemmer and R. Steinigeweg, *Entropy increase in k-step Markovian and consistent dynamics of closed quantum systems*, Phys. Rev. E **89**, 042113 (2014).
[67] D. Schmidtke and J. Gemmer, *Numerical evidence for approximate consistency and Markovianity of some quantum histories in a class of finite closed spin systems*, Phys. Rev. E **93**, 012125 (2016).
[68] C. Nation and D. Porras, *Taking snapshots of a quantum thermalization process: Emergent classicality in quantum jump trajectories*, Phys. Rev. E **102**, 042115 (2020).
[69] L. Diósi, *Anomalies of weakened decoherence criteria for quantum histories*, Phys. Rev. Lett. **92**, 170401 (2004).
[70] A. Smirne, D. Egloff, M. G. Díaz, M. B. Plenio, and S. F. Hulega, *Coherence and non-classicality of quantum Markov processes*, Quantum Sci. Technol. **4**, 01LT01 (2018).
[71] P. Strasberg and M. G. Díaz, *Classical quantum stochastic processes*, Phys. Rev. A **100**, 022120 (2019).
[72] S. Milz, F. Sakuldee, F. A. Pollock, and K. Modi, *Kolmogorov extension theorem for (quantum) causal modelling and general probabilistic theories*, Quantum **4**, 255 (2020).
[73] S. Milz, D. Egloff, P. Taranto, T. Theurer, M. B. Plenio, A. Smirne, and S. F. Huelga, *When is a non-Markovian quantum process classical?*, Phys. Rev. X **10**, 041049 (2020).
[74] P. Strasberg, *Quantum Stochastic Thermodynamics: Foundations and Selected Applications* (Oxford University Press, Oxford, 2022).
[75] P. Szańkowski and Ł. Cywiński, *Objectivity of classical quantum stochastic processes*, Quantum **8**, 1390 (2024).
[76] C. Emary, N. Lambert, and F. Nori, *Leggett-Garg inequalities*, Rep. Prog. Phys. **77**, 039501 (2014).
[77] C. Jess Riedel, *Living bibliography of the preferred basis problem*, https://blog.jessriedel.com/2020/07/18/living-bibliography-of-the-preferred-basis-problem/.
[78] A. Albrecht, *Investigating decoherence in a simple system*, Phys. Rev. D **46**, 5504 (1992).
[79] J. J. Halliwell, *Somewhere in the Universe: Where is the information stored when histories decohere?*, Phys. Rev. D **60**, 105031 (1999).
[80] P. J. Dodd and J. J. Halliwell, *Decoherence and records for the case of a scattering environment*, Phys. Rev. D **67**, 105018 (2003).
[81] J. B. Hartle, *Decoherent histories quantum mechanics starting with records of what happens*, arXiv:1608.04145.
[82] A. Schmid, *Repeated measurements on dissipative linear quantum systems*, Ann. Phys. (N.Y.) **173**, 103 (1987).
[83] J. J. Halliwell, *Approximate decoherence of histories and 't Hooft's deterministic quantum theory*, Phys. Rev. D **63**, 085013 (2001).
[84] Y. Subaşı and B. L. Hu, *Quantum and classical fluctuation theorems from a decoherent histories, open-system analysis*, Phys. Rev. E **85**, 011112 (2012).
[85] R. Omnès, *Logical reformulation of quantum mechanics. IV. Projectors in semiclassical physics*, J. Stat. Phys. **57**, 357 (1989).
[86] It is also worth noting that most of these indirect arguments aimed at establishing the DHC plus the fact that there is only a single history happening (i.e., a deterministic history framework). This is more than what is necessary in our view (the existence of classical stochastic processes is an experimental fact). Moreover, somewhat confusingly this stronger condition (DHC plus determinism) has been often called "quasiclassicality," which verbally suggests something weaker than classicality as used here. This is another reason for us to prefer the word decoherence over the word classicality.
[87] M. M. Wilde, *Quantum Information Theory*, 2nd ed. (Cambridge University Press, Cambridge, England, 2019).
[88] The factor "2" comes from the fact that the energy uncertainty of the projector $\Pi_{x,x'} \equiv \Pi_x^A \otimes \Pi_{x'}^B$ is $2\Delta E$ because both Π_x^A and $\Pi_{x'}^B$ have an energy uncertainty ΔE. Moreover, assuming H_{--}, H_{00}, and H_{++} to be diagonal can always be achieved by a block-unitary transformation. Finally, equal energy spacing is used for convenience only; a random spacing, for instance, has been observed to give rise to the same behavior.
[89] C. Bartsch, R. Steinigeweg, and J. Gemmer, *Occurrence of exponential relaxation in closed quantum systems*, Phys. Rev. E **77**, 011119 (2008).
[90] P. Strasberg and J. Schindler, *Shearing off the tree: Emerging branch structure and Born's rule in an equilibrated multiverse*, arXiv:2310.06755.
[91] A. Albrecht and L. Sorbo, *Can the Universe afford inflation?*, Phys. Rev. D **70**, 063528 (2004).
[92] S. M. Carroll, *Current controversies in philosophy of science* (Routledge, New York, 2020), ch. 1.
[93] M. P. Müller, *Law without law: From observer states to physics via algorithmic information theory*, Quantum **4**, 301 (2020).
[94] J. M. Deutsch, *Quantum statistical mechanics in a closed system*, Phys. Rev. A **43**, 2046 (1991).
[95] M. Srednicki, *Chaos and quantum thermalization*, Phys. Rev. E **50**, 888 (1994).
[96] M. Srednicki, *The approach to thermal equilibrium in quantized chaotic systems*, J. Phys. A **32**, 1163 (1999).
[97] P. Reimann and L. Dabelow, *Refining Deutsch's approach to thermalization*, Phys. Rev. E **103**, 022119 (2021).
[98] A. Kent, *Quantum histories*, Phys. Scr. **T76**, 78 (1998).
[99] J. J. Halliwell, *Commuting position and momentum operators, exact decoherence, and emergent classicality*, Phys. Rev. A **72**, 042109 (2005).
[100] M. B. Hastings, *Making almost commuting matrices commute*, Commun. Math. Phys. **291**, 321 (2009).
[101] Y. Ogata, *Approximating macroscopic observables in quantum spin systems with commuting matrices*, J. Funct. Anal. **264**, 2005 (2013).
[102] N. Y. Halpern, P. Faist, J. Oppenheim, and A. Winter, *Microcanonical and resource-theoretic derivations of the*

thermal state of a quantum system with noncommuting charges, Nat. Commun. **7**, 12051 (2016).

[103] A. Stokes and A. Nazir, *Gauge ambiguities imply Jaynes-Cummings physics remains valid in ultrastrong coupling QED*, Nat. Commun. **10**, 499 (2019).

[104] A. Stokes and A. Nazir, *Implications of gauge freedom for nonrelativistic quantum electrodynamics*, Rev. Mod. Phys. **94**, 045003 (2022).

[105] A. Kent, *Consistent sets yield contrary inferences in quantum theory*, Phys. Rev. Lett. **78**, 2874 (1997).

[106] R. B. Griffiths and J. B. Hartle, *Comment on "Consistent sets yield contrary inferences in quantum theory,"* Phys. Rev. Lett. **81**, 1981 (1998).

[107] A. Kent, *Kent replies*, Phys. Rev. Lett. **81**, 1982 (1998).

[108] L. He and W. G. Wang, *Statistically preferred basis of an open quantum system: Its relation to the eigenbasis of a renormalized self-Hamiltonian*, Phys. Rev. E **89**, 022125 (2014).

[109] D. Deutsch, *Many Worlds? Everett, Quantum Theory, and Reality* (Oxford University Press, Oxford, 2010), ch. 18, pp. 542–552.

[110] S. Aaronson, *Quantum Computing since Democritus* (Cambridge University Press, Cambridge, England, 2013).

[111] Y. Aharonov, P. G. Bergmann, and J. L. Lebowitz, *Time symmetry in the quantum process of measurement*, Phys. Rev. **134**, B1410 (1964).

[112] C. J. Isham, *Quantum logic and the histories approach to quantum theory*, J. Math. Phys. (N.Y.) **35**, 2157 (1994).

[113] C. J. Isham and N. Linden, *Information entropy and the space of decoherence functions in generalized quantum theory*, Phys. Rev. A **55**, 4030 (1997).

[114] L. Vaidman, *Many Worlds? Everett, Quantum Theory, and Reality* (Oxford University Press, Oxford, 2010), ch. 20, pp. 582–596.

[115] L. S. Schulman, *Opposite thermodynamic arrows of time*, Phys. Rev. Lett. **83**, 5419 (1999).

[116] O. Kupervasser, H. Nikolić, and V. Zlatić, *The universal arrow of time*, Found. Phys. **42**, 1165 (2012).

[117] S. M. Carroll and J. Chen, *Spontaneous inflation and the origin of the arrow of time*, arXiv:hep-th/0410270.

[118] J. Barbour, T. Koslowski, and F. Mercati, *Identification of a gravitational arrow of time*, Phys. Rev. Lett. **113**, 181101 (2014).

[119] J. M. Deutsch and A. Aguirre, *State-to-state cosmology: A new view on the cosmological arrow of time and the past hypothesis*, Found. Phys. **52**, 82 (2022).

[120] E. Calzetta and J. J. Gonzalez, *Chaos and semiclassical limit in quantum cosmology*, Phys. Rev. D **51**, 6821 (1995).

[121] N. J. Cornish and E. P. S. Shellard, *Chaos in quantum cosmology*, Phys. Rev. Lett. **81**, 3571 (1998).

[122] E. Calzetta, *Chaos, decoherence and quantum cosmology*, Classical Quantum Gravity **29**, 143001 (2012).

[123] J. Berjon, E. Okon, and D. Sudarsky, *Critical review of prevailing explanations for the emergence of classicality in cosmology*, Phys. Rev. D **103**, 043521 (2021).

[124] N. Dowling, P. Figueroa-Romero, F. A. Pollock, P. Strasberg, and K. Modi, *Relaxation of multitime statistics in quantum systems*, Quantum **7**, 1027 (2023).

[125] N. Dowling, P. Figueroa-Romero, F. A. Pollock, P. Strasberg, and K. Modi, *Equilibration of multitime quantum processes in finite time intervals*, SciPost Phys. Core **6**, 043 (2023).

[126] A. Aguirre and M. Tegmark, *Born in an infinite universe: A cosmological interpretation of quantum mechanics*, Phys. Rev. D **84**, 105002 (2011).

[127] L. Vaidman, *Derivations of the Born rule*, in *Quantum, Probability, Logic: The Work and Influence of Itamar Pitowsky*, edited by M. Hemmo and O. Shenker (Springer International Publishing, Cham, 2020), ch. 26, pp. 567–584.

[128] A. Albrecht and D. Phillips, *Origin of probabilities and their application to the multiverse*, Phys. Rev. D **90**, 123514 (2014).

[129] F. Del Santo and N. Gisin, *Physics without determinism: Alternative interpretations of classical physics*, Phys. Rev. A **100**, 062107 (2019).

[130] J. Wang and P. Strasberg, *Decoherence of histories: Chaotic versus integrable systems*, arXiv:2406.15577.